Iranian Journal of Astronomy and Astrophysics
Vol. 1, No. 1, 2013


**Iranian Journal of Astronomy and Astrophysics**

# Geomagnetic Field Effect over Azimuth Anisotropy of Cosmic Rays via Study of Primary Particles

Mehdi Khakian Ghomi[1] · Maedeh Fazlalizadeh[1] · Mahmoud Bahmanabadi[2] · Hadi Hedayati Kh.[3]

[1] Department of Physics, Amirkabir University of technology, P.O.Box 15875-4413, Tehran, Iran; email: mehdi.khakian@yahoo.com
[2] Department of Physics, Sharif University of technology, P.O.Box 11155-9161, Tehran, Iran
[3] Department of Physics, Khajenasir University of technology, Tehran, Iran

**Abstract**. Geomagnetic field is a one of the candidates for creation of anisotropy in azimuth distribution of extensive air showers over the entered cosmic rays to the atmosphere. Here we present the question: *Is there any azimuth anisotropy flux in the upper level of the atmosphere due to the geomagnetic field over the entered cosmic-rays?* The obtained answer is: *yes*. This investigation showed an agreement with a similar functionality to the experimental results, but its amplitude is smaller. We calculated the effect over the primary protons and alpha particles with consideration of their abundances, and found that this effect by itself is not as large as the expected value of experimental results. Therefore we need to investigate the secondary particles for the next step. But for a real simulation of extensive air showers, it is necessary to be applied this anisotropy flux as a seed for the secondary particle in the next step.

*Keywords*: Azimuth anisotropy, Cosmic Ray, Gamma Ray, Extensive Air Shower, Geomagnetic field

## 1 Introduction

We receive Cosmic-Rays(CRs) and Gamma-Rays(GRs) from celestial masses in addition to their light. In the energy range of a few TeV and more, CRs and GRs create Extensive Air Showers(EASs) that their secondary particles are detectable on the ground. Gamma ray sources are observable by the GR based EASs, the procedure which is used by Cherenkov Telescope Arrays like CANGAROO, H.E.S.S. , MAGIC, MILAGRO and VERITAS. But GR based EASs are only less than 1% of the EASs, so their contribution cannot explain the anisotropy distribution of the detected EASs in azimuth directions. Since the CR-distribution in TeV energy range inside the Galaxy is homogeneous, we expect an isotropic distribution in azimuth angles. But in the EAS detections; it is observed a slight North-South anisotropy flux of the CRs in the energy range, so it is expected a local effect over the EASs. There are so much attempts to understand the nature of the observed anisotropy in the EAS arrays [1, 2, 3]. Some analysis and calculations have been presented for explanations of it, like slope of the ground, time variations of the geomagnetic field, or dimension and direction of the field in the location of CR observations. But still non of the methods could not present a complete explanation for the anisotropy.
For a complete investigation it is needed to categorize the problem to smaller subproblems, like the geomagnetic field effect over *i)* primaries, *ii)* different secondaries separately and *iii)* investigation of group behavior of the secondaries as an EASs. Meanwhile there are many different works over shadow of the moon and the sun by EAS arrays. It has been well seen

that the sun's shadow is weaker than moon's [4]. It means that the effect over primaries is not negligible. The anisotropy is usually compared with a simple harmonic function with the first two harmonics:

$$A = N_0(1 + A_I \cos(x - \phi_I) + A_{II} \cos(2x - \phi_{II})) \quad (1)$$

In each point on the earth, we have two components of the geomagnetic field, one is to the nadir (zenith) in the north (south) hemisphere and the other is horizontal to the north (from the south). So we expect a complete period of $2\pi$ anisotropy in azimuth distribution everywhere. Also around the geomagnetic equator we have a symmetry in value of the field in North and South, therefore we expect a half period of $\pi$ anisotropy in azimuth distribution around the geomagnetic equator. It is interesting that $A_I$ ($A_{II}$) in equation 1 increases (decreases) with increase of observation latitude, which shows the North-South anisotropy [1, 3, 5]. At Tehran (35°.67 N, 51°.33 E, $\theta_H = 38°$) both $A_I$ and $A_{II}$ are important but always $A_I$ is larger than $A_{II}$. In Tibet array (30°.11 N, 90°.53 E, $\theta_H = 45°$) both $A_I$ and $A_{II}$are equally prevailing. At Yakutsk (62° N, 130° E, $\theta_H = 14°$) $A_I$ and in Chakaltaya (16°.35 S, 68°.20 W, $\theta_H = 16°$) $A_{II}$ are dominant [3]. Observations in different points show that the anisotropy amplitude is more in higher zenith angle events [1], and also is more in the results of higher latitude observatories. These results guides us to investigate the geomagnetic field as a good candidate for this phenomena [6]. Since the size of the geomagnetic field is about 50,000 nano-Tesla and its variations in a year is only about a few nano-Tesla (less than 50 nT/yr)(http://ngdc.noaa.gov), it seems that it is more wisely to investigate at first the effect of the geomagnetic field itself respect to its variations. This effect has been studied in the lower energies by A.M. Hillas [7] and J. Clay [8] for solar winds and investigations of van-allen belts and forbidden regions around the earth.
The geomagnetic field is approximately a dipole magnet which is located inside the Earth very near to the center, so its field has been expanded in a vast region around the Earth. Therefore the geomagnetic field at first; affects over primary CRs out of the atmosphere and then on secondary particles into the atmosphere. Energy of the primaries is very larger than the related secondaries, but the affecting time over the primaries is very larger than the secondaries. Dominant contribution of the North-South anisotropy can be due to *i)* deviation of primary CRs through the expanded geomagnetic field out of the atmosphere, *ii)* group deviation of created secondaries of an EAS inside the atmosphere or *iii)* both.
In this work we investigated the effect over primaries. In the second section we discuss about nature of the geomagnetic field and its effect over CRs. In the third section we present our calculation details of the effect over primaries. In the fourth section we show our results, and finally in the fifth section we present our discussion, concluding remarks and our agenda for the following works.

## 2 Geomagnetic Field

Geomagnetic field is due to a good approximate dipole magnet inside the earth which has an angle of 11°.5 with the earth rotation axis. Its magnetic moment is $8.1 \times 10^{25}$ Gs.cm$^3$ and shifted by 342 km relative to the earth center [9]. Magnetic north and south poles are at (83° N, 105° W) and (72° S, 110° W) respectively.
To check our magnetic dipole we used the calculator of "National Geography Data Center (NGDC: http://ngdc.noaa.gov)" for heights above Tehran (35°.67 N, 51°.33 E). For verification of the magnetic field at different heights, we considered Tehran location and obtained the field at different heights until 1000 km (the recommended region in NGDC for calculation of the magnetic field) by steps of 50 km. Figure 1 shows a very good agreement between

NGDC data and the dipole magnetic field. The results of the curve is used in the next steps of our calculations.

Since EASs secondary particles are creating inside the atmosphere with a very smaller

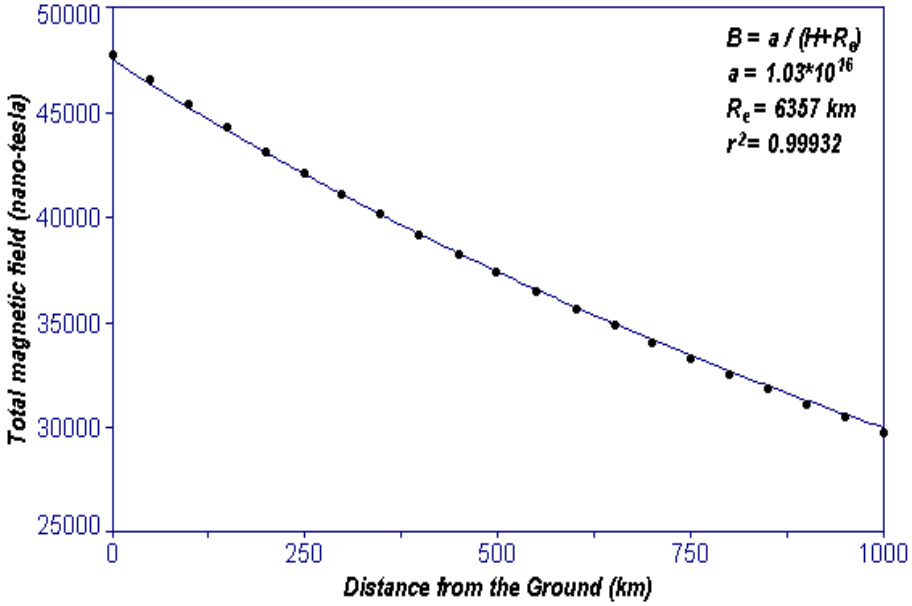


Figure 1: Magnetic field of the Earth, obtained from NGDC. It shows a good fit with dipole magnetic moment field ($B \propto 1/r^3$)[10] in different heights.

thickness relative to the dimensions of the earth magnetic atmosphere, therefore direction and size of the magnetic field is constant for secondaries [11], but this approximation is not true for primary particles. The field zone for the primaries is too vast to consider the geomagnetic factors constant, so they change with height, latitude and longitude which must be consider in our calculations.

# 3 Calculation Details of The Geomagnetic Field Effect over Primary Particles

In this stage we need a magnetic atmospheric zone. Since the geomagnetic field is a dipole magnet so $B \propto 1/r^3$ and in $r = 20,000$ km from earth center $B = (6,557/20,000)^3 B_0 \simeq 0.03B_0$. Therefore we define our magnetic atmosphere, a sphere around the earth with $r = 20,000$ km to the ground which most of the primary deviations are in the zone. Details of the deviation calculation of the primaries is presented as follows :

## 3.1 Calculation Details

Our reference coordinate system ($O$) is the equatorial coordinates but with longitude and complementary angle of latitude as spherical angles ($\beta$, $\pi/2 - \lambda$). Tehran's local coordinate system ($O'$) is; azimuth and zenith angles ($\phi$,$\theta$). Direction of the primary CRs in the local coordinates is $\mathrm{P}(\phi, \theta) = |\mathrm{P}| \sin\theta \cos\phi \hat{i}' + |\mathrm{P}| \sin\theta \sin\phi \hat{j}' + |\mathrm{P}| \cos\theta \hat{k}'$ where $\hat{i}'$,$\hat{j}'$ and $\hat{k}'$ are

unit vectors in $O'$ which are equivalent to $-\hat{\theta}$, $-\hat{\phi}$ and $\hat{r}$ in $O$ respectively (Figure 2). So $\mathrm{P}(\phi, \theta)$ in the equatorial coordinates is $\mathrm{P}(\beta, \lambda)$ :

$$\mathrm{P}(\beta, \lambda) = -|\mathrm{P}| \sin\theta \cos\phi\hat{\theta} - |\mathrm{P}| \sin\theta \sin\phi\hat{\phi} + |\mathrm{P}| \cos\theta\hat{r} \tag{2}$$

For determination of the inclination, we used *Lorentz Force* over the primary CRs from the starting point ($x_{max}$) to the upper level of atmosphere (8.4 km effectively) [12] and integrated over all of the path.
Maximum zenith angle in $O'$ coordinates is $\theta_{max} = 60^\circ$ [5], which is observable by our EAS array in Tehran (http://observatory.sharif.ir). Figure 2 shows the geometrical configuration of the two coordinates. An event with zenith angle $\theta$ in the local coordinates, has latitude $\lambda = (35 + \omega)^\circ$ where $\omega$ is central angle between $PO$ and $OO'$ in Figure 2.
With maximum amount of $x = x_{max} = 20,000$ km and $\theta = \theta_{max} = 60^\circ$ the highest latitude

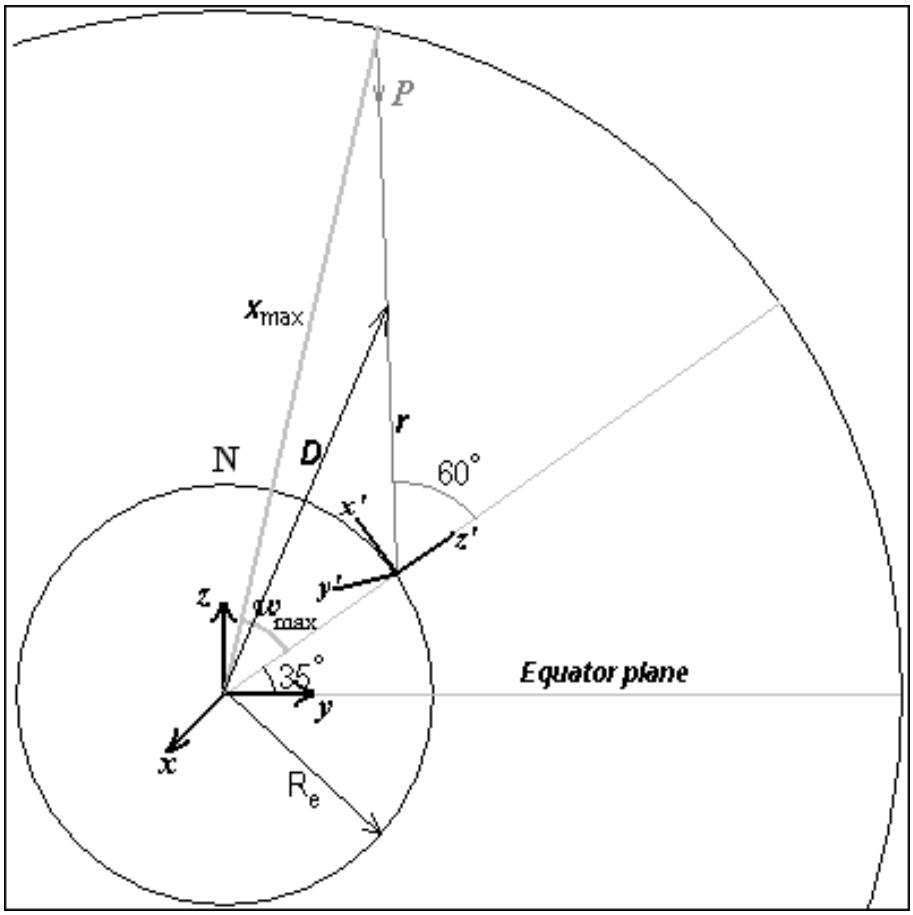


Figure 2: Geometry of the particles around the Earth. The particle comes to the magnetic atmosphere of the earth (x $\leq$ 20,000 km) and is affected by the magnetic field.

of the CRs is $\lambda_{max} = (35 + \omega_{max})^\circ$, which $\omega_{max} = \cos^{-1}((R_e + r_{max}\cos\theta_{max})/x_{max}) = 44^\circ$ where $R_e$ is the Earth radius. Therefore we need the magnetic field components in an area around Tehran with an angular radius of 44°.

We obtained $B_{x'}$, $B_{y'}$ and $B_{z'}$ in the intervals of $\lambda \subset [79, -9]$ and $\beta \subset [7, 95]$ by accuracy of 1°. Therefore we used integration differential $\delta r = r/44$ in the particle's path. In each step of the integration we subtracted $\delta r$ from distance of the particle to the upper level of atmosphere ($|\mathrm{r}| \longrightarrow |\mathrm{r}| - \delta r$), so $\lambda$, $\beta$ and $x$ change and in follow $B_{x'}$, $B_{y'}$ and $B_{z'}$ change too. Therefore P obtains :

$$\begin{aligned} \mathrm{P}(\phi, \theta; \beta, \lambda) = |\mathrm{P}| \sin\theta \cos\phi(\cos\lambda\cos\beta\hat{i} + \cos\lambda\sin\beta\hat{j} + \sin\lambda\hat{k}) \\ +|\mathrm{P}| \sin\theta \sin\phi(\sin\lambda\cos\beta\hat{i} + \sin\lambda\sin\beta\hat{j} - \cos\lambda\hat{k}) \\ +|\mathrm{P}| \cos\theta(-\sin\beta\hat{i} + \cos\beta\hat{j}) \end{aligned}$$

To find location of the particle in equatorial coordinates, in each step we obtained the vector $\mathbf{x} = \mathbf{r} + \mathbf{R_e}$ which $\mathbf{x}$ is the related vector of each step of the particle respect to the earth

$$\tan\beta = \rho_y/\rho_x \qquad , \qquad \tan\lambda = \sqrt{\rho_x^2 + \rho_y^2}/\rho_z \tag{3}$$

where $\rho_x$, $\rho_y$, $\rho_z$ and $x = (r^2 + R_e^2 + 2rR_e\cos\theta)^{1/2}$ are the components and size of the vector $\mathbf{x}$ in the equatorial coordinates. Consequently we will be able to calculate the size of $\mathbf{B}$ components $B(\beta, \lambda, x) = B(\beta, \lambda)(R_e/x)^3$ in each step. At the end of each step, for obtaining final momentum due to Lorentz force $\mathbf{F} = q(\mathbf{P} \times \mathbf{B})/\gamma m_0$, we calculated momentum differential $\Delta\mathbf{P} = \int \mathbf{F}dt$ where $dt = \delta r/c$. In the energy range it is clear that in each step angle between the particle's momentum and the geomagnetic field is constant, so we write $\Delta\mathbf{P} = \mathbf{F}\delta r/c$ and in the next step we have $\mathbf{P}(t + \Delta t) = \mathbf{P}(t) + \Delta\mathbf{P}$, and obtains a new direction. This process will continue until $x$ becomes smaller than the $x$ of Tehran's atmosphere ($R_e$+8.4 km), and at the end, final angles $(\phi_f, \theta_f)$ are given by $\mathbf{P}_f$ and the deflection angle obtains by comparison of $\mathbf{P}_i$ and $\mathbf{P}_f$.

# 4 Results

By using a *uniform* random generator for azimuth angles ($\phi_0$) of primaries and a "$\sin\theta_0$" random generator (Due to solid angle effect) for zenith directions ($\theta_0$). In our experiment the energy threshold ia about 40 TeV [5], so we used the energies from 1 to 100 TeV, and generated 5 sets of $1.5 \times 10^8$ events with energies of 1, 3, 10, 30 and 100 TeV. In each energy, we categorized the events with zenith angles in $0 - 10°$, $10° - 20°$, $\cdots$, $50° - 60°$ bins and azimuth angles in $0 - 30°$, $30° - 60°$, $\cdots$ $330° - 360°$ bins. The obtained results in different energies, zenith angles and azimuth angles distributions are presented respectively as follows :

## 4.1 Energy Dependence of the Anisotropy

For investigation of flux anisotropy in different azimuth angles, it is used the five large data sets and it is obtained azimuth deflection angle distribution for the data sets. In the investigation at first, we separated azimuth angle of the events in 12 of 30° bins, and then fitted the anisotropy function (equation 1) over the five energy sets of the simulated data. The results of the fittings has been presented in Table 1. In Figure 3 it is seen that the amplitude of the first harmonic is decreasing with increase of the primary energy. This means that the anisotropy amplitude in the first harmonic, decreases with increase of energy. But the difference is so small, it means that this effect is essentially very weak but it shows the right physical effect of the geomagnetic field over higher and lower energies. Since the

fluctuations in the obtained ensemble ($\Delta\phi = \phi_f - \phi_i$) is high, we see large error bars, but all of the events in the data sets averagely show a very fine right physical effect.

Table 1: Anisotropy coefficients of equation 1 in different energies for all zenith angles, $E$ is the primary particle energy

| $E\ (TeV)$ | $N_0(\times 10^7)$ | $A_I(\times 10^{-4})$ | $\phi_I(^\circ)$ | $A_{II}(\times 10^{-4})$ | $\phi_{II}(^\circ)$ |
|---|---|---|---|---|---|
| 1 | 1.24962 | 1.89511 | 190.19 | 2.88129 | 95.04 |
| 3 | 1.24962 | 1.86892 | 187.74 | 2.98770 | 94.38 |
| 10 | 1.24962 | 1.85640 | 188.71 | 2.92697 | 91.87 |
| 30 | 1.24962 | 1.85222 | 190.86 | 2.98020 | 94.10 |
| 100 | 1.24962 | 1.83365 | 188.81 | 3.06506 | 96.72 |

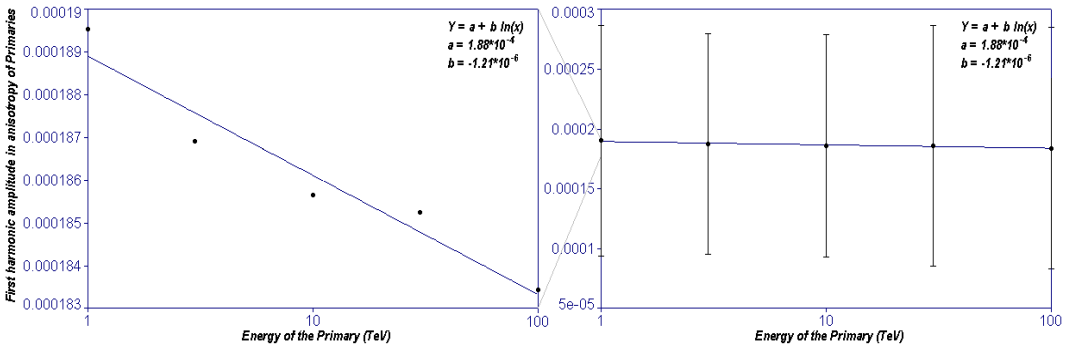


Figure 3: Amplitude of the first harmonic function over azimuth distribution of the simulated events, for 5 differerent energies: 1, 3, 10, 30 and 100 TeV.

## 4.2 Deflection Angle vs. Primary Zenith Angle

Deflection angle of the particles are obtained by comparing direction of the primary particle before and after passing through the geomagnetic field. As we expected the deflection angle $\gamma$ ($\cos\gamma = \cos\theta_0\cos\theta_f + \sin\theta_0\sin\theta_f\cos(\phi_f - \phi_0)$) increases with increase of $\theta_0$. The best fit for the deflection angle vs. zenith angle of the events obtained by function "$\gamma = \mathbf{a} + \mathbf{b}\theta^{\mathbf{c}}$" over the obtained data. It is seen that in different energies, the variations of **a**, **b** and **c** is very small (Table 2), which is in agreement with the results of section 4.1. These results have been averaged over the simulated events for each angle interval. As an example, Figure 4 shows the distribution for 100 TeV events. The results in the *total* row of the Table 2 show that this effect is actually weak-sensitive respect to the energy of the primaries, which is in agreement with the first result.

## 4.3 North-South Anisotropy

Figure 5 shows a North-South anisotropy respect to the geomagnetic north ($11^\circ.5\ N$) in azimuth ($\phi$) angles of the primary particles. The anisotropy is obtained for the five data sets and obtained a very small variation in $\Delta\phi = \phi_f - \phi_i$. In the experiments we have a deficit in North part and an excess in South [1, 2, 3]. If we compare this result with

Table 2: It is seen a similar behavior of deflection angle of the primaries in different energies in the geomagnetic field with increase of zenith angle. $a$, $b$ and $c$ are fitting constants of the function $\gamma = a + b\theta^c$.

| $E\ (TeV)$ | a | b | c | $r^2$ |
|---|---|---|---|---|
| 1 | 19.19 | 0.235 | 1.232 | 0.99369 |
| 3 | 19.09 | 0.253 | 1.214 | 0.99283 |
| 10 | 19.54 | 0.206 | 1.264 | 0.99277 |
| 30 | 19.45 | 0.221 | 1.247 | 0.99189 |
| 100 | 19.19 | 0.235 | 1.232 | 0.99253 |
| *total* | $19.29(1 \pm 0.01)$ | $0.230(1 + 0.07)$ | $1.238(1 \pm 0.01)$ | |

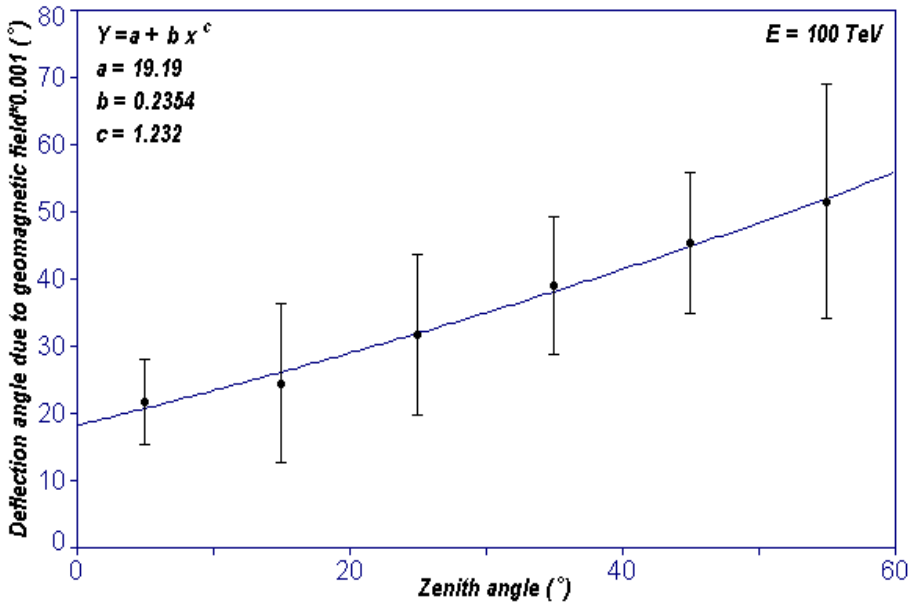


Figure 4: Deviation of the primary particles after passing through the geomagnetic field vs. zenith angle of the events for $E = 100$ TeV. Black points and error bars are average and standard deviations in each angle interval.

the experimental results, it is seen that there is a $\pi$ phase difference between them. The result is quite right because we drew the deflection angle and in north part we see maximum deflection which shows maximum deficit, and in south part we se minimum deflection which shows a pile up due to deflection from border events in the neighbor bins.

## 5 Discussion and Concluding Remarks

It is seen that in the experiments results, the observed anisotropy (amplitude of the first or second harmonics) is about few percent, but in the investigation the anisotropy due to the geomagnetic field over primary particles is very smaller than the amount that we expect. It is about %0.01 about hundred times smaller. If it is payed attention to the title of y-axis of

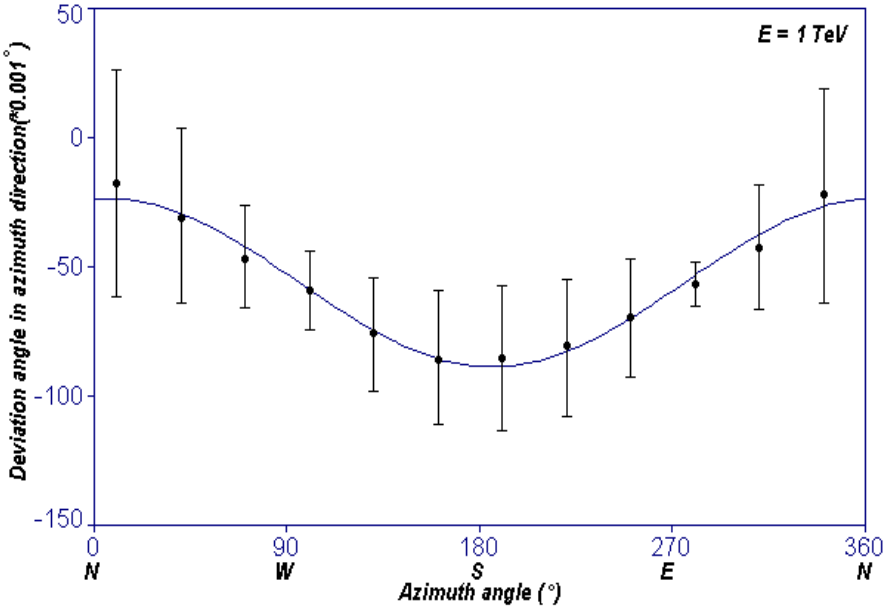


Figure 5: Average azimuth deviation in different azimuth directions which shows a North-South anisotropy.

figure 4 and 5 we have a coefficient of 0.001°. This shows a very small angular deflection, consequently the anisotropy difference in different energies is small too. From Table 1 it is seen that the relative amplitude difference in different energies ($\Delta A_i$, $i = I$, $II$) to the amplitudes ($A_i$) is about 0.01, so observation of any variations in different energies from 1 $TeV$ to 100 $TeV$ is not so easy. In this investigation we see that the anisotropy due to the primary particles shows expectable physical behavior (functionalities) but is smaller than our expected experimental results.
Usually for the estimation of angular resolution of EAS arrays the moon and sun shadow are investigated [4]. In most of the works it is observed a weaker and broader shadow of the sun respect to the moon. Usually presented a reason for the phenomena which is the magnetic field of the sun (which affects over primaries). Usually it is seen that the angular size of the sun's shadow is about few degrees. If we compare the $x_{max} \sim 20,000$ km respect to the sun-earth distance$\sim 150 \times 10^6$ km it is about 7 to 8 thousand times. Therefore we can expect that the deflection is about the order of thousandth of degrees.
Hence for the next agenda we investigate the geomagnetic field effect over the secondary particles of EASs and their group behavior with consideration of the obtained anisotropy as a seed for their primaries.

## Acknowledgment

This research was supported by a grant from office of vice president for science, research and technology of Amirkabir University of Technology (Tehran Polytechnic).
I thank Dr. Paolo Bernardini for his so much constructive advises for understanding the geomagnetic field problem over EASs.
Also I thank Prof. G. Schutz for his constructive comments.

## References

[1] Ivanov A. A., Egorova V. P., Kolosov V. A., Krasilnikov A. D., Pravdin M. I., Sleptsov H. Y., 1999, JETP letters, 69(4), 288

[2] He H. H., Bernardini P., Calabrese Melcarne A. K., Chen S. Z., 2007, Astropart. Phys., 27, 528

[3] Bahmanabadi M., Anvari A., Khakian Ghomi M., Pourmohammad D., Samimi J., Lamehi Rachti M., 2002, Experimental Astronomy, 13, 39

[4] Oshima A., Gupta S. K., Hayashi K., et al., 2008, Proc. 30th ICRC, Mexico, **3**, (OG part 2), 1515-1518

[5] Khakian Ghomi M., Bahmanabadi M., Samimi J., 2005, A&A, 434, 459

[6] Khakian Ghomi M., Bahmanabadi M., Samimi J., Shadkam A.H., Sheydaei F., Anvari A., 2007, Proc. 30th ICRC, Yukatan Mexico, HE11-0263

[7] Hillas A. M., 1972, Cosmic Rays. Pergamon Press, p. 22

[8] Clay J., 1972, Proc. Roy. Acad., Amsterdam, Vol. 30, p. 1115

[9] Dorman L. I., 2008, Cosmic Rays in Magnetospheres of the Earth and other Planets, Spriger, P. 9

[10] Reitz J. R., Milford F. J., Christy R. W., 1979, Foundations of Electromagnetic Theory, 3rd edition, Adison Wesley

[11] He H. H., Bernardini P., Calabrese Melcarne A. K., Chen S. Z., 2005, Proc. 29th ICRC, Pune India, Vol. 6, P. 5

[12] Gaisser T.K., 1990, Cosmic Rays and particle Physics, cambridge University Press New York, p. 35